Assessing the applicability of quantum corrections to classical thermal conductivity predictions

J. E. Turney,[1] A. J. H. McGaughey,[1,*] and C. H. Amon[1,2]

[1]*Department of Mechanical Engineering, Carnegie Mellon University, Pittsburgh, Pennsylvania 15213, USA*
[2]*Department of Mechanical and Industrial Engineering, University of Toronto, Toronto, Ontario, Canada M5S 3G8*

The validity of the commonly used quantum corrections for mapping a classically predicted thermal conductivity onto a corresponding quantum value are assessed by self-consistently predicting the classical and quantum thermal conductivities of a crystalline silicon system via lattice-dynamics calculations. Applying the quantum corrections to the classical predictions, with or without the zero-point energy, does not bring them into better agreement with the quantum predictions compared to the uncorrected classical values above temperatures of 200 K. By examining the mode dependence of the phonon properties, we demonstrate that thermal conductivity cannot be quantum corrected on a system level. We explore the source of the differences in the quantum and classical phonon relaxation times on a mode-by-mode basis.

I. INTRODUCTION

Classical molecular-dynamics (MD) simulation is a powerful tool for predicting physical behavior and material properties.[1–3] As a general rule, MD simulations of solids are considered valid near and above a material's Debye temperature, where all of the vibrational modes (i.e., phonons in a crystal) are fully excited. Molecular-dynamics simulations are not valid at lower temperatures, where quantum effects cannot be neglected. To mitigate this limitation, quantum corrections (QCs) have been developed. The purpose of QCs is to map predictions made for a classical system onto corresponding values in a quantum system. Quantum corrections have been derived from first principles for thermodynamic, mechanical, and structural properties (e.g., Helmholtz free energy, entropy, bulk modulus, and pair-distribution function).[4–6] Rigorous QCs for transport properties such as thermal conductivity are more difficult to obtain.[7]

The commonly used QCs for thermal conductivity are based on *ad hoc* physical arguments rather than fundamental theory. These QCs are applied to the temperature T and the thermal conductivity k.[8,9] The temperature correction is made by equating the total energies of the classical and quantum systems. The energy equality can be expressed as

$$\sum_{\boldsymbol{\kappa},\nu}^{N,3n} E^{\mathrm{C}}\begin{pmatrix}\boldsymbol{\kappa}\\\nu\end{pmatrix} = \sum_{\boldsymbol{\kappa},\nu}^{N,3n} E^{\mathrm{Q}}\begin{pmatrix}\boldsymbol{\kappa}\\\nu\end{pmatrix}, \qquad (1)$$

where the sums are over all phonon modes denoted by N wave vectors $\boldsymbol{\kappa}$ and $3n$ dispersion branches ν, $E\begin{pmatrix}\boldsymbol{\kappa}\\\nu\end{pmatrix}$ is the energy of a phonon mode, and the superscripts C and Q indicate classical and quantum. By assuming (i) equipartition of the classical energy and subtracting the three translational degrees of freedom, and (ii) the quantum energy to be harmonic, Eq. (1) becomes

$$3(Nn-1)k_{\mathrm{B}}T^{\mathrm{C}} = \sum_{\boldsymbol{\kappa},\nu}^{N,3n}\left[\hbar\omega\begin{pmatrix}\boldsymbol{\kappa}\\\nu\end{pmatrix}f^{\mathrm{Q}}\begin{pmatrix}\boldsymbol{\kappa}\\\nu\end{pmatrix} + \frac{\hbar\omega\begin{pmatrix}\boldsymbol{\kappa}\\\nu\end{pmatrix}}{2}\right]. \quad (2)$$

Here, k_{B} is the Boltzmann constant, $\hbar$ is the Planck constant divided by 2π, and $\omega\begin{pmatrix}\boldsymbol{\kappa}\\\nu\end{pmatrix}$ and $f\begin{pmatrix}\boldsymbol{\kappa}\\\nu\end{pmatrix}$ are the mode-dependent

frequency and equilibrium occupation number. For the quantum system, the equilibrium occupation number follows the Bose-Einstein distribution,

$$f^{\mathrm{Q}} = \frac{1}{\exp\left(\frac{\hbar\omega}{k_{\mathrm{B}}T^{\mathrm{Q}}}\right) - 1}. \qquad (3)$$

The term $\hbar\omega\begin{pmatrix}\boldsymbol{\kappa}\\\nu\end{pmatrix}/2$ in Eq. (2) is the zero-point (ZP) energy. The ZP energy has no parallel in a classical system and, as will be shown, plays an important role in the QCs. Equation (2) cannot be explicitly solved for T^{Q} but T^{Q} can be determined by computing T^{C} for a series of T^{Q} values and then interpolating.

The thermal conductivity correction is

$$k^{\mathrm{Q}} = k^{\mathrm{C}}\frac{dT^{\mathrm{C}}}{dT^{\mathrm{Q}}}, \qquad (4)$$

which arises from equating the heat fluxes obtained from the Fourier law in the classical and quantum systems. The QCs given by Eqs. (2) and (4) have been applied to classical MD thermal conductivity predictions for amorphous silicon,[9] crystalline silicon in bulk[10–12] and thin films,[13] β-silicon carbide,[14] silicon-germanium superlattices,[15] carbon nanotubes,[16] and transition metals (the phonon contribution).[17]

The validity of Eqs. (2) and (4) is questionable as they are not derived from fundamental relations and have not been rigorously tested. The doubts regarding these QCs are further exemplified by the nonconsensus on whether to include the ZP energy in Eq. (2) or to ignore it.[18] The objective of this work is to rigorously assess the validity of the QCs for thermal conductivity given by Eqs. (2) and (4). To do so, we self-consistently predict the classical and quantum thermal conductivities of crystalline silicon via lattice-dynamics (LD) calculations and then apply the QCs to the classical predictions. We find that the QCs are not valid and demonstrate why by using phonon properties obtained from the LD calculations.

II. LATTICE-DYNAMICS METHOD FOR PREDICTING PHONON PROPERTIES

We predict the classical and quantum thermal conductivities of an ordered (i.e., crystalline) material in a self-consistent manner using LD calculations. Consider a crystal with N lattice sites and an n-atom unit cell with periodic boundary conditions applied in all directions. Harmonic LD is first used to find the phonon frequencies and polarization vectors $\mathbf{e}$ (i.e., the normal modes of vibration) under the harmonic approximation by solving the eigenvalue problem

$$\omega^2 \begin{pmatrix} \boldsymbol{\kappa} \\ \nu \end{pmatrix} \mathbf{e} \begin{pmatrix} \boldsymbol{\kappa} \\ \nu \end{pmatrix} = \mathbf{D}(\boldsymbol{\kappa}) \mathbf{e} \begin{pmatrix} \boldsymbol{\kappa} \\ \nu \end{pmatrix}. \tag{5}$$

The dynamical matrix $\mathbf{D}(\boldsymbol{\kappa})$ has dimension $3n \times 3n$ and elements

$$
\begin{aligned}
&D_{3(b-1)+\alpha, 3(b'-1)+\alpha'}(\boldsymbol{\kappa}) \\
&= \frac{1}{\sqrt{m_b m_{b'}}} \sum_{l'}^{N} \left. \frac{\partial^2 \Phi}{\partial r_\alpha \begin{pmatrix} 0 \\ b \end{pmatrix} \partial r_{\alpha'} \begin{pmatrix} l' \\ b' \end{pmatrix}} \right|_o \\
&\times \exp \left\{ i\boldsymbol{\kappa} \cdot \left[\mathbf{r} \begin{pmatrix} l' \\ b' \end{pmatrix} - \mathbf{r} \begin{pmatrix} 0 \\ b \end{pmatrix} \right] \right\},
\end{aligned}
\tag{6}
$$

where b and α index over the atoms in the unit cell and the Cartesian coordinates, Φ is the total potential energy, $\mathbf{r}\binom{l}{b}$ is the average position vector for the bth atom in the lth unit cell with $r_\alpha\binom{l}{b}$ as its α component, and m is the atomic mass.[19,20]

The harmonic phonon frequencies and polarization vectors are then used as input to an anharmonic LD calculation to compute the mode-dependent phonon frequency shifts Δ and linewidths Γ. For a quantum system these two quantities are determined for mode 0 (i.e., $\boldsymbol{\kappa}_0$ and ν_0) from[21,22]

$$
\begin{aligned}
\Delta_0^Q &= \frac{\hbar}{16N} \sum_{\boldsymbol{\kappa}_1, \nu_1}^{N,3n} \sum_{\boldsymbol{\kappa}_2, \nu_2}^{N,3n} \left| \Phi \begin{pmatrix} \boldsymbol{\kappa}_0 & \boldsymbol{\kappa}_1 & \boldsymbol{\kappa}_2 \\ \nu_0 & \nu_1 & \nu_2 \end{pmatrix} \right|^2 \{[f_1^Q + f_2^Q + 1] \\
&\times [(\omega_0 - \omega_1 - \omega_2)_p^{-1} - (\omega_0 + \omega_1 + \omega_2)_p^{-1}] \\
&+ [f_1^Q - f_2^Q][(\omega_0 + \omega_1 - \omega_2)_p^{-1} - (\omega_0 - \omega_1 + \omega_2)_p^{-1}]\} \\
&- \frac{\hbar}{8N} \sum_{\boldsymbol{\kappa}_1, \nu_1}^{N,3n} \sum_{\nu_2}^{3n} \Phi \begin{pmatrix} -\boldsymbol{\kappa}_0 & \boldsymbol{\kappa}_0 & 0 \\ \nu_0 & \nu_1 & \nu_2 \end{pmatrix} \Phi \begin{pmatrix} -\boldsymbol{\kappa}_1 & \boldsymbol{\kappa}_1 & 0 \\ \nu_0 & \nu_1 & \nu_2 \end{pmatrix} \\
&\times [2f_1^Q + 1](\omega_2)_p^{-1} + \frac{\hbar}{8N} \sum_{\boldsymbol{\kappa}_1, \nu_1}^{N,3n} \Phi \begin{pmatrix} \boldsymbol{\kappa}_0 & \boldsymbol{\kappa}_1 & -\boldsymbol{\kappa}_0 & -\boldsymbol{\kappa}_1 \\ \nu_0 & \nu_1 & \nu_0 & \nu_1 \end{pmatrix} \\
&\times [2f_1^Q + 1],
\end{aligned}
\tag{7}
$$

and

$$
\begin{aligned}
\Gamma_0^Q &= \frac{\pi \hbar}{16N} \sum_{\boldsymbol{\kappa}_1, \nu_1}^{N,3n} \sum_{\boldsymbol{\kappa}_2, \nu_2}^{N,3n} \left| \Phi \begin{pmatrix} \boldsymbol{\kappa}_0 & \boldsymbol{\kappa}_1 & \boldsymbol{\kappa}_2 \\ \nu_0 & \nu_1 & \nu_2 \end{pmatrix} \right|^2 \\
&\times \{[f_1^Q + f_2^Q + 1]\delta(\omega_0 - \omega_1 - \omega_2) \\
&+ [f_1^Q - f_2^Q][\delta(\omega_0 + \omega_1 - \omega_2) - \delta(\omega_0 - \omega_1 + \omega_2)]\},
\end{aligned}
\tag{8}
$$

Property	Quantum	Classical
f	$\dfrac{1}{\exp(x)-1}$	$\dfrac{1}{x}$
c_{ph}	$\dfrac{k_B x^2 \exp(x)}{V[\exp(x)-1]^2}$	$\dfrac{k_B}{V}$
$v_{g,x}$	$\dfrac{\partial \omega_A}{\partial \kappa_x}$	$\dfrac{\partial \omega_A}{\partial \kappa_x}$
τ	$\dfrac{1}{2\Gamma}$	$\dfrac{1}{2\Gamma}$

where $(\ )_p$ and $\delta(\ )$ denote the Cauchy principal value and Dirac delta function, and ω_1 implies $\omega\binom{\boldsymbol{\kappa}_1}{\nu_1}$. The term $\Phi\binom{\boldsymbol{\kappa}_0 \boldsymbol{\kappa}_1 \cdots \boldsymbol{\kappa}_j}{\nu_0 \nu_1 \cdots \nu_j}$ contains the jth-order derivative of the potential energy evaluated at the average atomic positions (i.e., the jth-order force constant) and is

$$
\begin{aligned}
&\Phi \begin{pmatrix} \boldsymbol{\kappa}_0 \boldsymbol{\kappa}_1 \cdots \boldsymbol{\kappa}_j \\ \nu_0 \nu_1 \cdots \nu_j \end{pmatrix} \\
&= \sum_{\alpha_0, b_0}^{3,n} \sum_{\alpha_1, b_1, l_1}^{3,n,N} \cdots \sum_{\alpha_j, b_j, l_j}^{3,n,N} \delta_{(\boldsymbol{\kappa}_0 + \boldsymbol{\kappa}_1 + \cdots + \boldsymbol{\kappa}_j), \mathbf{K}} \\
&\times \left. \frac{\partial^j \Phi}{\partial r_{\alpha_0}\begin{pmatrix} 0 \\ b_0 \end{pmatrix} \partial r_{\alpha_1}\begin{pmatrix} l_1 \\ b_1 \end{pmatrix} \cdots \partial r_{\alpha_j}\begin{pmatrix} l_j \\ b_j \end{pmatrix}} \right|_o \\
&\times \frac{e_0\begin{pmatrix} b_0 \\ \alpha_0 \end{pmatrix} e_1\begin{pmatrix} b_1 \\ \alpha_1 \end{pmatrix} \cdots e_j\begin{pmatrix} b_j \\ \alpha_j \end{pmatrix}}{[m_{b_0}\omega_0 m_{b_1}\omega_1 \cdots m_{b_j}\omega_j]^{1/2}} \exp\left[i\boldsymbol{\kappa}_0 \cdot \mathbf{r}\begin{pmatrix} 0 \\ b_0 \end{pmatrix} \right] \\
&\times \exp\left[i\boldsymbol{\kappa}_1 \cdot \mathbf{r}\begin{pmatrix} l_1 \\ b_1 \end{pmatrix} \right] \cdots \exp\left[i\boldsymbol{\kappa}_j \cdot \mathbf{r}\begin{pmatrix} l_j \\ b_j \end{pmatrix} \right],
\end{aligned}
\tag{9}
$$

where $e_j\binom{b_j}{\alpha_j}$ is the eigenvector component associated with atom b_j and the α_j direction. The Kronecker delta $\delta_{(\boldsymbol{\kappa}_1 + \boldsymbol{\kappa}_2 + \cdots + \boldsymbol{\kappa}_j), \mathbf{K}}$ is one if the sum of the wave vectors is a reciprocal-lattice vector $\mathbf{K}$ and zero otherwise. We use Eqs. (7) and (8) to evaluate the frequency shifts and linewidths for a classical system by substituting $f^C - 1/2$ in place of f^Q. The expressions for the phonon occupation number for quantum and classical harmonic oscillators are given in Table I.

The thermal conductivity is then evaluated using the relation

$$k = \sum_{\boldsymbol{\kappa}} \sum_{\nu} c_{ph}\begin{pmatrix} \boldsymbol{\kappa} \\ \nu \end{pmatrix} v_{g,x}^2 \begin{pmatrix} \boldsymbol{\kappa} \\ \nu \end{pmatrix} \tau \begin{pmatrix} \boldsymbol{\kappa} \\ \nu \end{pmatrix}, \tag{10}$$

which is derived from the Boltzmann transport equation under the relaxation-time approximation, and is valid for both the quantum and classical systems.[23] Expressions for the phonon specific heat c_{ph}, x component of the group velocity $v_{g,x}$, and relaxation time τ are given in Table I.

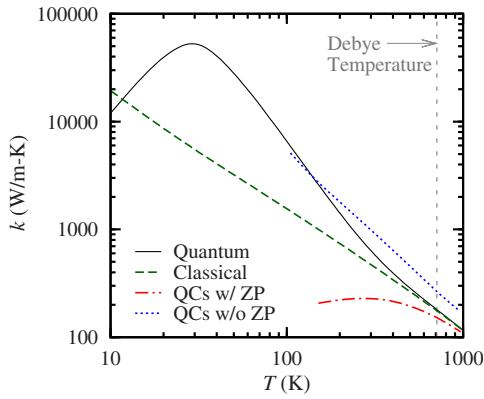We will use the LD method to predict the thermal conductivity of isotopically pure crystalline silicon modeled

FIG. 1. (Color online) Thermal conductivity predictions for the quantum and classical systems and the quantum-corrected classical prediction using the ZP energy (QCs with ZP) and neglecting it (QCs without ZP).

FIG. 2. (Color online) Phonon linewidths ($\Gamma = \frac{1}{2\tau}$) plotted versus harmonic frequency for quantum and classical systems at a temperature of 100 K.

with the Stillinger-Weber (SW) interatomic potential[24] between temperatures of 10 and 1000 K. While the low-temperature approximations inherent in the LD techniques cause them to loose accuracy at high temperature, the quantum and classical thermal conductivity predictions remain self-consistent.[23] The thermal conductivity predictions only account for phonon-phonon scattering and neglect other scattering mechanisms, such as impurity and boundary scattering, which would be present in a real sample. We perform the calculations on the eight-atom unit cell arrayed on a simple cubic $N_0 \times N_0 \times N_0$ lattice. We set the lattice parameter to 5.43 Å, which is within 0.4% of the MD-predicted lattice parameters at all temperatures considered.[25] To achieve size-independent thermal conductivity predictions, we use $N_0 = 12$ for temperatures above 100 K and $N_0 = 30$ for lower temperatures. Further details about LD theory and our implementation of the LD method for predicting thermal conductivity are given by Turney *et al.*[23]

III. ASSESSING THE QUANTUM CORRECTIONS

A. Quantum and classical thermal conductivity

The SW silicon thermal conductivities predicted using the LD method are plotted in Fig. 1 for the quantum and classical systems between temperatures of 10 and 1000 K. The quantum and classical predictions converge at high temperature, as they must. The low-temperature thermal conductivity behavior is also as expected. The quantum thermal conductivity peaks at a temperature of 30 K then approaches zero as the temperature goes to zero. The classical thermal conductivity prediction increases monotonically as the temperature decreases and diverges to infinity at zero temperature. For temperatures less than 100 K, phonon scattering from defects, isotopes, and boundaries is important.[26] We have neglected these scattering mechanisms, resulting in very large thermal conductivity values at these temperatures. We note that Broido *et al.*[26] predicted the thermal conductivity of SW silicon using an approach related to the LD method presented here with these additional scattering mechanisms included.

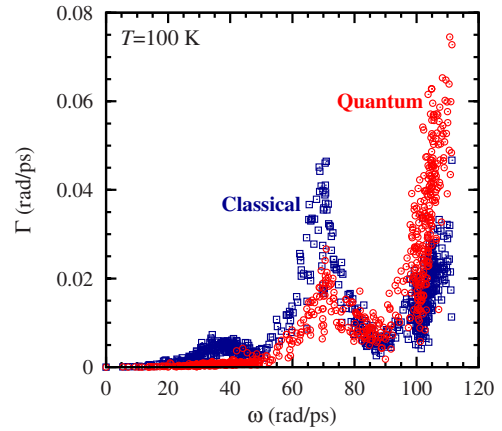For temperatures above 15 K, the classical thermal conductivities are less than the quantum values. This result is not necessarily intuitive because the classical phonon specific heats are always greater than their quantum counterparts and, according to Eq. (10), will tend to increase the classical thermal conductivity over the quantum value. The thermal conductivity, however, is also affected by the group velocities and the relaxation times. Because SW silicon is a stiff material, the group velocities for the quantum and classical systems are nearly identical and show weak temperature dependence. The relaxation times, however, have a large impact.

Plotted in Fig. 2 are the phonon linewidths ($\frac{1}{2\tau}$) versus harmonic frequency at a temperature of 100 K. At frequencies below 80 rad/ps, the quantum phonons have smaller linewidths than the classical phonons. At higher frequencies, the situation is reversed. Considering the equation for the linewidth [Eq. (8)], we see that two types of phonon interactions contribute to Γ_0. One is the decay of the phonon ω_0 into two phonons ($\omega_0 \to \omega_1 + \omega_2$, a type-I interaction). The other is the annihilation of the phonon with a second to create a third ($\omega_0 + \omega_1 \to \omega_2$ or $\omega_0 + \omega_2 \to \omega_1$, a type-II interaction). The differences between the quantum and classical linewidths are driven by the occupation numbers, f^Q and f^C, which weight the phonon interactions. For the quantum and classical systems, the type-I interactions are weighted by $f_1^Q + f_2^Q + 1$ and $f_1^C + f_2^C$. Of these two weighting factors, the quantum expression is always greater than the classical expression for the same set of frequencies at the same temperature. The type II weighting factor for the quantum system, $f_1^Q - f_2^Q$, is always less than its classical counterpart, $f_1^C - f_2^C$. We note that energy conservation, enforced by the Dirac delta functions in Eq. (8), causes type-I interactions to dominate when ω_0 is large, resulting in quantum linewidths that are greater than their classical counterparts. When ω_0 is small, type-II interactions dominate, giving rise to quantum linewidths that tend to be smaller than the classical values. At intermediate frequencies, both type-I and type-II interactions play an important role. This discussion illustrates an important point, which is that the relaxation time for a single-phonon mode depends strongly on the other phonon modes in the system.

To explore the consequences of the different relaxation times on the thermal conductivity, consider Fig. 3 where the ratio of the mode-dependent thermal conductivities, k_{ph}^Q / k_{ph}^C
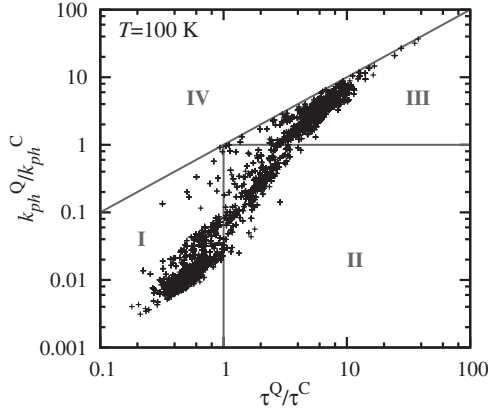
FIG. 3. Ratio of the quantum to classical phonon thermal conductivities plotted versus the relaxation-time ratio for all phonon modes at a temperature of 100 K.

$[=c_{ph}^{Q}(v_{g,x}^{Q})^2\tau^{Q}/c_{ph}^{C}(v_{g,x}^{C})^2\tau^{C}]$, is plotted against the ratio of the relaxation times τ^{Q}/τ^{C} at a temperature of 100 K. We identify four regions separated by the lines $k_{ph}^{Q}/k_{ph}^{C}=1$, $\tau^{Q}/\tau^{C}=1$, and $k_{ph}^{Q}/k_{ph}^{C}=\tau^{Q}/\tau^{C}$. Region IV is inaccessible because the quantum specific heat is always lower than the classical specific heat. In regions I and II, the mode-dependent quantum thermal conductivity is lower than the classical value, despite the quantum relaxation time being larger than the classical relaxation time in region II. For phonon modes in region III, the quantum relaxation time is so much larger than the classical value that it negates the reduction caused by the specific heat. The net result in this region is that the mode-dependent quantum thermal conductivity is larger than the classical value. For temperatures above 15 K, the phonons in region III dominate the thermal transport, causing the total quantum thermal conductivity to be greater than the classical prediction (see Fig. 1).

B. Quantum-corrected thermal conductivity

The temperature mapping from the classical system to the quantum system defined by Eq. (2) is plotted in Fig. 4 when the ZP energy is both considered and neglected. Also plotted
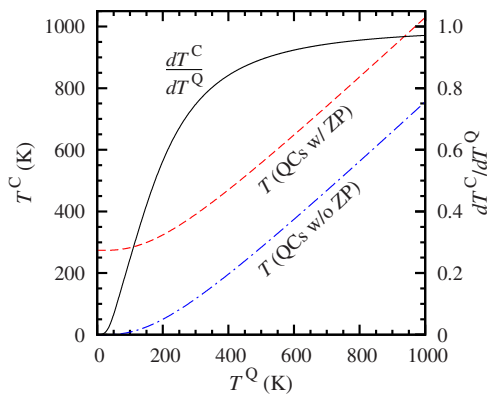

FIG. 4. (Color online) Mapping between quantum and classical temperatures with and without the ZP energy and dT^{C}/dT^{Q} as defined by Eqs. (2) and (4).

is the scaling factor dT^{C}/dT^{Q} defined by Eq. (4). This factor is independent of the ZP energy and is always less than one. The scaling factor can be written as

$$\frac{dT^{C}}{dT^{Q}} = \frac{1}{3(Nn-1)k_{B}} \sum_{\kappa,\nu}^{N,3n} c_{ph}^{Q}\begin{pmatrix}\kappa \\ \nu\end{pmatrix}, \qquad (11)$$

which is obtained by differentiating Eq. (2) with respect to T^{Q} and assuming the phonon frequencies to be temperature independent. The temperature mapping depends strongly on the inclusion or exclusion of the ZP energy. For the same quantum temperature, the classical temperatures for the two cases are offset by the average ZP energy divided by k_{B}, which is 270 K for SW silicon. When the ZP energy is included, the corrected temperature is greater than the quantum temperature, the corrected and quantum temperatures converge in the high-temperature (i.e., classical) limit, and a classical system below a temperature of 270 K has no quantum counterpart. When the ZP energy is excluded, the corrected temperature is less than the quantum temperature and the corrected and quantum temperatures do not converge in the high-temperature limit but are separated by 270 K.

The effect of the QCs on the classical thermal conductivity prediction is shown in Fig. 1, where we plot the quantum-corrected classical predictions. Neglecting the ZP energy increases the thermal conductivity. Including the ZP energy causes the thermal conductivity to shift downward away from the quantum predictions.

For QCs to be valid, the corrected classical predictions must (i) converge to the quantum predictions at high temperature and (ii) provide a better estimation of the quantum thermal conductivity than the uncorrected classical predictions. Our four sets of results (quantum, classical, and two sets of quantum-corrected classical values) do converge at high temperature, although the convergence is slow for both sets of quantum-corrected values. At the SW silicon Debye temperature of 710 K,[27] the corrected thermal conductivities with and without the ZP energy are 10% lower and 30% higher than the quantum value while the uncorrected classical prediction is within 5% of the quantum value. At a temperature of 300 K, less than half the Debye temperature, the classical prediction is still within 15% of the quantum value. For temperatures above 200 K, neither of the QC approaches improves upon the agreement between the uncorrected classical value and the quantum value.

When including the ZP energy, a maximum in the thermal conductivity is predicted. The location and magnitude of this maximum, however, are clearly wrong. The lowest uncorrected temperature we consider is 10 K, which corresponds to a temperature of 105 K for the QCs without the ZP energy. The quantum-corrected thermal conductivity predictions without the ZP energy can be extended to lower temperatures by fitting a power function to the uncorrected classical predictions and extrapolating. In doing so (not shown), we find that the quantum-corrected thermal conductivity does not exhibit a maximum when the ZP energy is neglected. From these observations, we conclude that the QCs prescribed by Eqs. (2) and (4), with the ZP energy either included or ne-
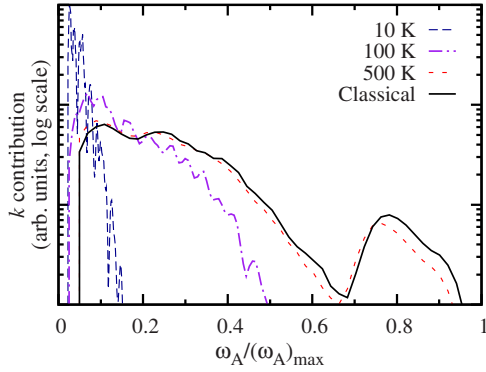
FIG. 5. (Color online) Scaled contribution to the thermal conductivity as a function of frequency ratio. The classical results at all temperatures collapse to a single curve.

glected, do not properly account for quantum effects. These QCs even fail at high temperatures, where quantum effects are small.

C. Analyzing the quantum corrections

The reasons why the QCs given by Eqs. (2) and (4) fail can be deduced by considering the mode dependence of the phonon properties (ω, c_{ph}, $v_{g,x}$, and τ). In Fig. 5, we plot the contribution to the thermal conductivity versus phonon frequency, both scaled by their maximum values, for temperatures of 10, 100, and 500 K. When plotted this way, the results for the classical systems collapse to a single temperature-independent curve. For the quantum system, however, the low-frequency phonons increasingly dominate the thermal conductivity as the temperature decreases. This effect is due to the temperature dependence of the occupation number [Eq. (3)], which effectively freezes out the high-frequency modes at low temperatures. Applying the QCs given by Eqs. (2) and (4) shifts the thermal conductivity by a temperature-dependent scale factor. Yet, we see from Fig. 5 that the frequency dependence of the mode contribution is strongly temperature dependent. The thermal conductivity thus cannot be properly corrected by applying a system-level scaling factor.

We can further address the reasons why the QCs fail by investigating what would need to be done to properly correct a classically predicted thermal conductivity. From the discussion in the previous paragraph, we know that QCs must be performed on the level of the phonon modes [i.e., the terms inside the summation in Eq. (10)]. To simplify the analysis, we retain the assumption of a temperature-independent lattice constant and further assume the frequency shift to be negligible. This assumption is good for SW silicon as the root mean square of Δ/ω is less than 0.03 for all temperatures considered. When the frequency shift is neglected, the group velocity becomes temperature independent, and is the same in the quantum and classical systems. The phonon specific heats and relaxation times, however, differ between the two systems. If these two mode-dependent properties can be properly quantum corrected, then we would be able to predict a quantum thermal conductivity from classical phonon

properties. In what follows, we will assume that all the classical phonon properties are known. Although not typically found in a Green-Kubo[28,29] or direct[28,30] MD-based thermal conductivity prediction, these phonon properties can be obtained from MD simulations.[23,31]

Correcting the specific heat is straightforward. The classical specific heat is a constant and the quantum specific heat can be computed from the phonon frequency (see Table I). The first step in converting the classical thermal conductivity to a quantum thermal conductivity thus involves scaling the contribution of each phonon mode by c_{ph}^{Q}/c_{ph}^{C}.[32] From Eq. (11), we see that the quantum correction defined by Eq. (4) is on the right track in that it scales the classical thermal conductivity by the ratio of the quantum specific heat to the classical specific heat. This scaling, however, is performed on the system level rather than on the level of the phonon modes, as is required.

The relaxation times cannot be corrected in the same manner. Using the LD approach described in Sec. II, the effort required to compute quantum relaxation times is the same as the effort required to compute classical relaxation times. Additionally, if the quantum relaxation times were known, we could compute the quantum thermal conductivity directly using Eq. (10).

What we would like is for the classical relaxation times to be representative of the relaxation times of a corresponding quantum system. We determine the quantum system represented by the classical relaxation times by setting $\tau^Q = \tau^C$ for each phonon mode, which is equivalent to letting $\Gamma^Q = \Gamma^C$. The equation for the quantum linewidth [Eq. (8)] can be converted to a classical linewidth by setting

$$f^C = f^Q + 1/2. \tag{12}$$

This condition links the quantum and classical systems. Solving Eq. (12) for T^Q, we find the temperature of a quantum system that has the same occupation number as the classical system to be

$$T^Q = \frac{\hbar\omega}{k_B \ln\left[\dfrac{2k_B T^C + \hbar\omega}{2k_B T^C - \hbar\omega}\right]}. \tag{13}$$

We can immediately see a problem with Eq. (13). The quantum temperature is a function of the phonon frequency, meaning that the classical relaxation times cannot be mapped onto an equilibrium quantum system at a single temperature. The quantum temperature corresponding to classical temperatures of 100, 420, 710, and 1000 K is plotted versus frequency in Fig. 6. Above the Debye temperature (710 K), the range of quantum temperatures associated with the classical temperature is small. The classical relaxation times at these temperatures are a good approximation of the quantum relaxation times and there is no need to perform a quantum correction. As the classical temperature decreases below the Debye temperature, the range of quantum temperatures increases and the classical relaxation times are not indicative of the relaxation times of an equilibrium quantum system. When the classical temperature drops below 420 K, some of the high-frequency phonon modes cannot be mapped onto
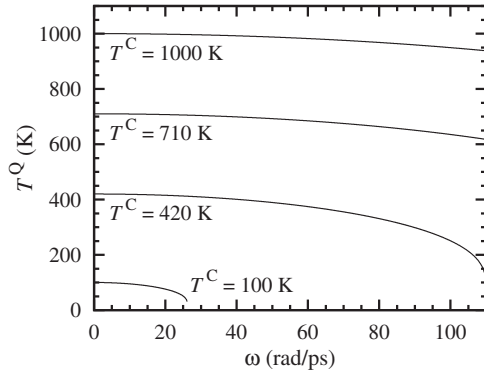
FIG. 6. Frequency-dependent quantum temperatures as determined by Eq. (12) for various classical temperatures. For temperatures less than 420 K, some of the high-frequency phonons cannot be mapped into any quantum system.

any quantum system. Although they make a small direct contribution to the thermal conductivity, these high-frequency phonons are important in that they scatter with low-frequency phonons. These mapping issues are also inherent in Eq. (2) (where T^Q is found as a weighted average) and contribute to the failure of the QCs.

D. Discussion

Others have argued for the QCs given by Eqs. (2) and (4) because they can bring classical MD thermal conductivity predictions into better agreement with experimental measurements. When examining all the available data, however, we find that some find better agreement when the ZP energy is considered[13,14,16,32] while others find better agreement when the ZP energy is ignored.[11,12] Based on the results presented in Sec. III B, we believe that any improved agreement is fortuitous as MD-predicted thermal conductivities are sensitive to the chosen interatomic potential. Interatomic potentials are an approximation of the complex interactions that exist between atoms, which only quantum calculations (e.g., density-functional theory) can accurately capture. Using an approach related to the LD method presented here, Broido and co-workers[26] found that a fully quantum-mechanical treatment of SW silicon does not match the experimental thermal conductivity data while the same treatment using input from density-functional-theory calculations does.[33]

Alternative approaches for obtaining a quantum thermal conductivity prediction from classical MD simulations have been suggested. These approaches are based on modifying the MD simulation itself, making them fundamentally different than QCs, which are a postprocessing procedure. Li[34] suggested initializing a classical MD simulation with a phonon distribution corresponding to a quantum system at equilibrium. Wang[35] proposed a classical MD simulation that interacts with heat baths that are forced to maintain quantum phonon distributions. The drawback of these approaches is that the MD simulation is limited temporally or spatially. A system with an initial quantum configuration will eventually relax to an equilibrium classical state. A large MD system in contact with quantum heat baths will have a classical phonon distribution far from the heat baths.

Quantum MD simulation (e.g., Car-Parrinello[36]) in conjunction with the Green-Kubo or direct method has not been used to predict thermal conductivity because it is too computationally expensive. A less computationally expensive approach is to use Feynman path integrals to effectively transform a quantum system into a classical system, whose static properties can then be computed using classical MD or Monte Carlo simulations.[37] Centroid MD, an extension of path-integral MD developed by Cao and Voth,[38,39] has been used to predict transport properties of quantum systems, such as thermal conductivity and shear viscosity.[40]

Fully quantum-mechanical predictions of thermal conductivity, made using the LD method employed here or a related method developed by Omini and Sparavigna,[41,42] are an excellent alternative to MD-based predictions for ordered systems well below the Debye temperature, where the weakly interacting phonon model is valid. Lattice-dynamics-based predictions of the thermal conductivity have the additional advantages of allowing their input to come from density-functional-theory calculations and providing the complete phonon properties.[23] At higher temperatures, quantum effects are unimportant and classical MD-based methods are suitable if an accurate interatomic potential is available.

IV. CONCLUSIONS

We have assessed the validity of the commonly used QCs for thermal conductivity [Eqs. (2) and (4)] by using harmonic and anharmonic LD calculations to self-consistently predict the quantum and classical thermal conductivities of SW silicon. Applying the QCs to the classical predictions, with or without the ZP energy, does not bring them into better agreement with the quantum predictions compared to the uncorrected classical values above temperatures of 200 K (see Fig. 1). When neglecting the ZP energy, the quantum-corrected temperature does not approach the quantum temperature in the high-temperature limit and there is no maximum in the thermal conductivity. When the ZP energy is included, the corrected thermal conductivity shifts away from the quantum prediction, and the location and magnitude of the maximum do not agree with the quantum results. Although not presented here, we have seen the same behavior in Lennard-Jones argon.

By examining the frequency dependence of the thermal conductivity (see Fig. 5), we found that system-level properties, such as those used in Eqs. (2) and (4), cannot be used to bring classical thermal conductivities into agreement with quantum values. While the specific heat can be quantum corrected on a mode-by-mode basis, the system temperature cannot be quantum corrected because the phonons in a classical system are not representative of the phonons in an equilibrium quantum system at a single temperature (see Fig. 6). Differences between the classical and quantum relaxation times (see Figs. 2 and 3) can be attributed to the frequency dependence of the occupation numbers and the dominant scattering mechanism. The mapping of classical phonons onto an equivalent quantum system is approximately correct only at high temperatures, where QCs are unnecessary.

*Corresponding author; mcgaughey@cmu.edu

[1] M. P. Allen and D. J. Tildesley, *Computer Simulation of Liquids* (Oxford University Press, Oxford, 1987).

[2] D. C. Rapaport, *The Art of Molecular Dynamics Simulation* (Cambridge University Press, Cambridge, 1995).

[3] A. J. H. McGaughey and M. Kaviany, in *Advances in Heat Transfer*, edited by G. Greene, Y. Cho, J. Hartnett, and A. Bar-Cohen (Elsevier, New York, 2006), Vol. 39, pp. 169–255.

[4] P. H. Berens, D. H. J. Mackay, G. M. White, and K. R. Wilson, J. Chem. Phys. **79**, 2375 (1983).

[5] M. Matsui, J. Chem. Phys. **91**, 489 (1989).

[6] V. A. Levashov, S. J. L. Billinge, and M. F. Thorpe, J. Comput. Chem. **28**, 1865 (2007).

[7] J. Che, T. Cagin, W. Deng, and W. A. Goddard III, J. Chem. Phys. **113**, 6888 (2000).

[8] C. Z. Wang, C. T. Chan, and K. M. Ho, Phys. Rev. B **42**, 11276 (1990).

[9] Y. H. Lee, R. Biswas, C. M. Soukoulis, C. Z. Wang, C. T. Chan, and K. M. Ho, Phys. Rev. B **43**, 6573 (1991).

[10] A. Maiti, G. D. Mahan, and S. T. Pantelides, Solid State Commun. **102**, 517 (1997).

[11] S. G. Volz and G. Chen, Phys. Rev. B **61**, 2651 (2000).

[12] S. Volz and G. Chen, Physica B **263-264**, 709 (1999).

[13] C. J. Gomes, M. Madrid, J. V. Goicochea, and C. H. Amon, ASME Trans. J. Heat Transfer **128**, 1114 (2006).

[14] J. Li, L. Porter, and S. Yip, J. Nucl. Mater. **255**, 139 (1998).

[15] S. Volz, J. B. Saulnier, G. Chen, and P. Beauchamp, Microelectron. J. **31**, 815 (2000).

[16] J. R. Lukes and H. Zhong, ASME Trans. J. Heat Transfer **129**, 705 (2007).

[17] P. Heino, Phys. Scr., T **T114**, 171 (2004).

[18] A. J. H. McGaughey, Ph.D. thesis, University of Michigan, 2004.

[19] M. T. Dove, *Introduction to Lattice Dynamics* (Cambridge University Press, Cambridge, England, 1993).

[20] A. J. H. McGaughey, M. I. Hussein, E. S. Landry, M. Kaviany, and G. M. Hulbert, Phys. Rev. B **74**, 104304 (2006).

[21] D. C. Wallace, *Thermodynamics of Crystals* (John Wiley & Sons, New York, 1972).

[22] A. A. Maradudin and A. E. Fein, Phys. Rev. **128**, 2589 (1962).

[23] J. E. Turney, E. S. Landry, A. J. H. McGaughey, and C. H. Amon, Phys. Rev. B **79**, 064301 (2009).

[24] F. H. Stillinger and T. A. Weber, Phys. Rev. B **31**, 5262 (1985).

[25] J. Goicochea, M. Madrid, and C. Amon, ASME Trans. J. Heat Transfer (to be published).

[26] D. A. Broido, A. Ward, and N. Mingo, Phys. Rev. B **72**, 014308 (2005).

[27] E. S. Landry and A. J. H. McGaughey, Phys. Rev. B **79**, 075316 (2009).

[28] P. K. Schelling, S. R. Phillpot, and P. Keblinski, Phys. Rev. B **65**, 144306 (2002).

[29] H. Kaburaki, J. Li, S. Yip, and H. Kimizuka, J. Appl. Phys. **102**, 043514 (2007).

[30] J. Lukes, D. Li, X.-G. Liang, and C.-L. Tien, ASME Trans. J. Heat Transfer **122**, 536 (2000).

[31] A. J. H. McGaughey and M. Kaviany, Phys. Rev. B **69**, 094303 (2004).

[32] J. V. Goicochea, Ph.D. thesis, Carnegie Mellon University, 2008.

[33] D. A. Broido, M. Malorny, G. Birner, N. Mingo, and D. A. Stewart, Appl. Phys. Lett. **91**, 231922 (2007).

[34] J. Li, Ph.D. thesis, Massachusetts Institute of Technology, 2000.

[35] J.-S. Wang, Phys. Rev. Lett. **99**, 160601 (2007).

[36] R. Car and M. Parrinello, Phys. Rev. Lett. **55**, 2471 (1985).

[37] D. M. Ceperley, Rev. Mod. Phys. **67**, 279 (1995).

[38] J. Cao and G. A. Voth, J. Chem. Phys. **100**, 5093 (1994).

[39] J. Cao and G. A. Voth, J. Chem. Phys. **100**, 5106 (1994).

[40] Y. Yonetani and K. Kinugawa, J. Chem. Phys. **119**, 9651 (2003).

[41] M. Omini and A. Sparavigna, Physica B **212**, 101 (1995).

[42] M. Omini and A. Sparavigna, Phys. Rev. B **53**, 9064 (1996).